Experimental Investigation on the Effect of Central Wavelength Tuning of FBG-Based Phase Shifter for Raman-Assisted Phase Sensitive Amplifier

Y. Cao[(1)], H. Song[(1)], Y. Akasaka[(2)], A. Almaiman[(1)], A. Mohajerin-Ariaei[(1)], C. Bao[(1)], P. Liao[(1)], F. Alishahi[(1)], A. Fallahpour[(1)], T. Ikeuchi[(2)], D. Starodubov[(1)], J. Touch[(1, 3)], A. E. Willner[(1)]

[(1)] Department of Electrical Engineering, University of Southern California, Los Angeles, CA 90089, USA, yinwenca@usc.edu
[(2)] Fujitsu Laboratories of America, 2801 Telecom Parkway, Richardson, TX 75082, USA
[(3)] Information Sciences Institute, University of Southern California, Marina del Rey, CA 90292, USA

Abstract *A FBG-based pump-phase-shifter is used in the Raman-assisted PSA. By actively tuning the FBG central-wavelength to enable pump phase optimization, up-to-5.6dB signal gain is observed. An improvement of ~6% EVM and ~4dB system sensitivity is observed by 20/25-Gbaud QPSK signals.*

Introduction

Capacity upgrade utilizing higher level modulation formats such as 64QAM and 256QAM has been studied aggressively. Such higher level formats need sufficient OSNR to maintain the transmission reach. Phase sensitive amplifier (PSA) is one of potential candidates due to the below 3dB noise figure[1,2].

In order to achieve the optimal performance of PSA, an optical phase shifter is necessary to ensure phase matching among PSA pump, signal and idler, which could be realized by a waveshaper. However, the insertion loss of a typical waveshaper might decrease the PSA gain by reducing the power of both signal and pump. On the other hand, Bragg grating has many applications such as tunable filter[3], chromatic dispersion compensator[4] and sensor[5-7]. In addition, a Fiber Bragg grating (FBG) with 0.4dB insertion loss has been used as a pump-phase-shifter in a Raman-assisted PSA system, where more than 20dB signal net gain has been experimentally demosntrated[8]. However, in the previous research, the FBG central wavelength is fixed. Therefore, once the pump wavelength is determined, the FBG induced phase shift is also fixed. This is a potential limitation for the practical implementation, in which phase matching condition may degrade due to some reasons such as system component aging. Therefore, it might be valuable to actively tune the FBG central wavelength, enabling more flexible pump phase adjustment.

In this paper, the temperature of a FBG-based phase shifter is tuned to investigate the effect of FBG central wavelength shift on the phase matching condition in the Raman-assisted PSA system. A FBG central wavelength shift up to 0.66nm is observed when increasing the temperature by 60°C. With FBG central wavelength tuning, up to 5.6dB signal gain improvement is observed. For a 20 Gbaud QPSK signal, the EVM is decreased by ~6%. In addition, ~4dB system sensitivity improvement is experimentally demonstrated for both 20/25 Gbaud QPSK signals.

Concept and Experimental Setup

Figure 1 shows the conceptual diagram. In order to suppress the noise on the signal wavelength at the idler generation stage, the PSA pump power is adjusted to have moderate conversion efficiency (~-10dB). The power imbalance is compensated by the higher Raman gain on the idler (I) which is achieved by placing signal (S) away from Raman gain profile. By locating PSA pump wavelength close to the FBG central (Bragg) wavelength but detuning from FBG bandwidth, only the phase of PSA pump can be affected by the FBG. Based on the thermoelectric effect, current injection changes the temperature of FBG, which in turn shifts the FBG central wavelength to optimize the phase of PSA pump. Therefore, the phase matching condition is achieved in the following PSA stages, enabling optimized system performance.

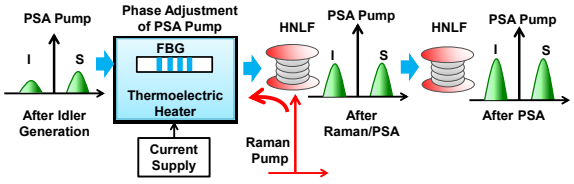

Fig. 1: Concept of Raman-assisted PSA enabled by the FBG-based phase shifter. The phase adjustment of PSA pump is achieved by FBG central wavelength tuning based on thermoelectric effect. The power imbalance between signal and idler is compensated by placing the signal away from Raman gain profile.

Figure 2(a) shows the experimental setup. At the transmitter, the signal modulates a laser at the wavelength of 1569.8nm through a QPSK modulator. An attenuator (ATT-1) is placed afterwards to change the input signal power to the system. A PSA pump at the wavelength of

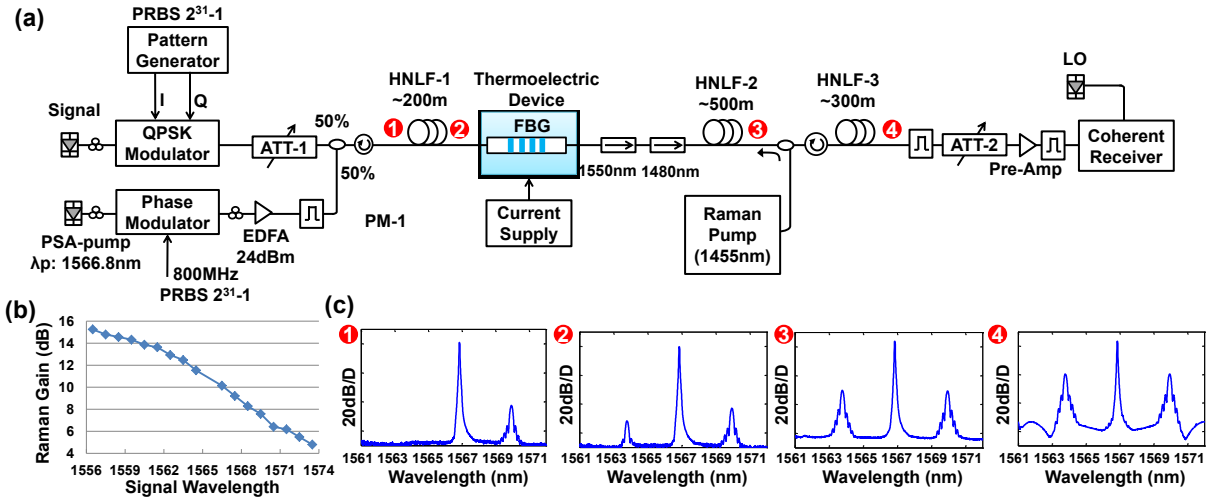

Fig. 2: (a) Experimental setup; (b) unflattened Raman gain profile to decrease the power imbalance between the signal and the idler; (c) optical spectra corresponding to each node. PRBS: pseudorandom binary sequence; HNLF: highly nonlinear fiber; ATT: attenuator; FBG: fiber Bragg grating; LO: local oscillator.

1566.8nm is phase modulated by an 800Mhz pseudorandom binary sequence (PRBS) to suppress the stimulated Brillouin scattering (SBS) effect. Then, the signal and the PSA pump are coupled by a 50/50 coupler followed by a circulator to monitor SBS and any power reflection from the FBG. The wavelength of PSA pump is carefully adjusted to ensure that it stays close to the FBG central wavelength but doesn't fall into the reflection region.

In the first stage, the signal and the PSA pump are sent through a 200m highly nonlinear fiber (HNLF-1) with nonlinear coefficient of 21.4 $W^{-1}km^{-1}$, zero dispersion wavelength (ZDW) of 1551.5nm and a dispersion slope of $0.043ps/km/nm^2$. It is noted that all three HNLFs in the expeiment have similar parameters. After HNLF-1, an idler with -10dB conversion efficiency is generated with negligible parametric gain on the signal. Then, a 15mm FBG with 0.4dB loss and maximum reflectivity of -37dB is heated by a thermoelectric device. For example, a 0.8amps current can change the temperature by 60°C to shift the FBG central wavelength by 0.66nm, enabling phase adjustment of the PSA pump. In the next stage, the signal, idler and PSA pump are amplified by a counter-propagated Raman pump at the wavelength of 1455nm in a 500m HNLF (HNLF-2). Figure 2(b) shows that longer wavelength gets less Raman gain; therefore, the 10dB power imbalance of the signal (longer wavelength) and the idler (shorter wavelength) could be compensated by the unflattened Raman gain profile together with four wave mixing (FWM). In the third stage, all the components are sent to a 300m HNLF (HNLF-3) and the signal gets a further PSA gain. After that, the signal is selected and sent to another attenuator (ATT-2) for pre-amplification before the coherent receiver. The system spectra corresponding to each node are shown in Fig. 2(c). The periodic peaks and dips in Fig. 2(c4) might be caused by the single-mode-fiber (SMF) pigtail and this oscillation could be removed by direct splicing.

Results and Discussions

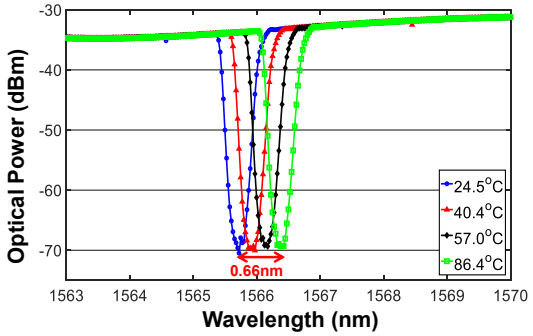

Fig. 3: FBG central wavelength tuning by changing the temperature of FBG.

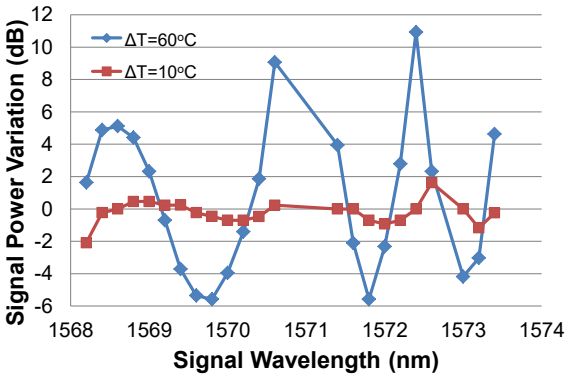

Fig. 4: The variation of output signal power with different FBG temperature changes.

By tuning the FBG temperature based on thermoelectric effect, the central wavelength of FBG is shifted as shown in Fig. 3, in which a 60°C temperature difference provides a 0.66nm shift. The shifted FBG central wavelength changes the phase of PSA pump, which affects the signal amplification by PSA accordingly. Figure 4 shows the variation of the signal output power with the FBG temperature tuning. When the temperature change (ΔT) increases, the

variation of output signal power becomes severe.

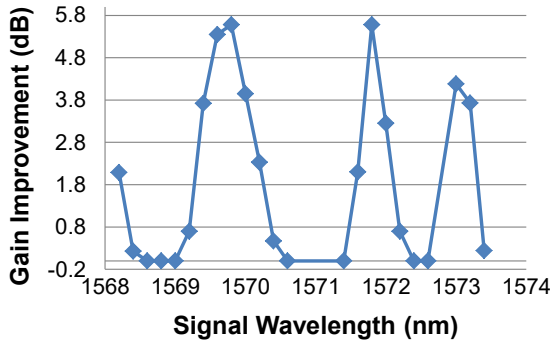

Fig. 5: Gain improvement by optimizing FBG central wavelength for the signal at different wavelength.

Then, the signal wavelength is swept and the PSA pump phase is optimized for each wavelength. Compared to the case without FBG central wavelength tuning, the signal has an extra gain because of the achieved phase matching condition. Due to the system dispersion, the optimal pump phase for each wavelength is different. As shown in Fig. 5, for some wavelengths such as 1568.6nm, the FBG central wavelength in the room temperature already provides optimal pump phase. Therefore, the gain improvement by FBG tuning is 0. However, for other wavelengths such as 1569.8nm, FBG central wavelength tuning can bring more than 5dB gain improvement.

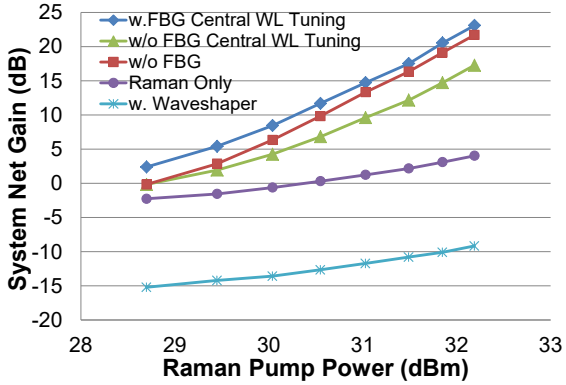

Fig. 6: System net gain comparison for different scenarios.

In Fig. 6, a comparison of the system net gain for different scenarios by varying the Raman pump power is carried with the signal wavelength of 1569.8nm. Without PSA pump, the signal gain is entirely from Raman amplification and the system net gain is below 5dB. By turning on the PSA pump the system net gain can reach 23dB and 17dB with and without FBG central wavelength tuning, respectively. It is noted that when the FBG is taken out of the system, the system gain is only 1.5dB less than the FBG optimized system. The potential reason might attribute to the 0.4dB FBG insertion loss which not only decreases the signal power but also attenuates the PSA pump power. In addition, we replace the FBG with a waveshaper. Because of much higher insertion loss (13.5dB), only negative gain is observed.

In the following, the constellation of a 20 Gbaud QPSK signal at 1569.8nm is compared among different scenarios as shown in Fig. 7. For the comparison, the input signal power before the pre-amplifier at the receiver is fixed at -20.47dBm by adjusting the attenuator (ATT-2) in Fig. 2. Figure 7 shows FBG tuning can bring ~6% EVM improvement compared to that without FBG tuning. In addition, ~2% EVM improvement is obtained even though a FBG-free system has less system loss. System BER performance is compared in Fig. 8(a), in which a 4dB sensitivity benefit is observed with FBG tuning. Compared to the FBG-free case, there is still a 1.5dB sensitivity improvement. Figure 8(b) shows the BER performance comparison for a 25 Gbaud QPSK system, in which similar system improvement is observed.

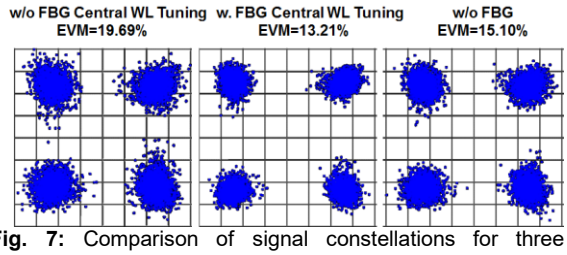

Fig. 7: Comparison of signal constellations for three scenarios: (1) without FBG central wavelength tuning; (2) with FBG central wavelength tuning; (3) without FBG.

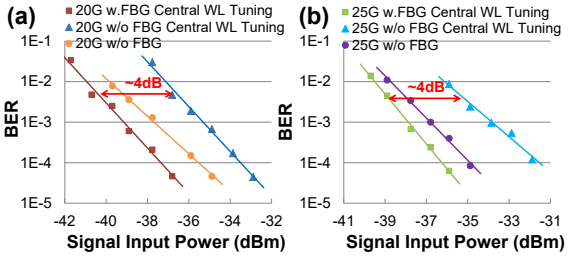

Fig. 8: Comparison of measured BER versus the input power of 20/25 Gbaud QPSK signals for three scenarios: (1) without FBG central wavelength tuning; (2) with FBG central wavelength tuning; (3) without FBG.

Acknowledgements

The authors would like to thank the support of CIAN, Fujitsu Laboratories of America, Furukawa Electric Co. LTD and NSF.

References

[1] Z. Tong et al., Nat. Photon., Vol. **5**, p. 430 (2011).

[2] M. Ettabib et al., Opt. Exp., Vol. **20**, p. 1629 (2012).

[3] A. Iocco et al., J. Lightw. Technol, vol. **17**, p. 1217(1999).

[4] M. Sumetsky et al., J. Opt. Fiber Commun. Rep., vol. **2**, p. 256 (2005).

[5] C. Caucheteur et al., Photon. Technol. Lett., vol. **20**, p. 96 (2008).

[6] A. Ricchiuti et al., Opt. Exp., Vol. **21**, p. 28175 (2013).

[7] M. Rosenberger et al., Sensors, vol. **15**, p. 4264 (2015).

[8] Y. Cao et al., Proc. OFC, Th4A.2, Los Angeles (2017).